Quantitative Proteomics Analysis of the Effects of Ionizing Radiation in Wild Type and p53^{K317R} Knock-in Mouse Thymocytes*▣

Lisa M. Miller Jenkins‡, Sharlyn J. Mazur‡, Matteo Rossi‡, Olga Gaidarenko§, Yang Xu§, and Ettore Appella‡¶

The tumor suppressor protein p53 is a sequence-specific transcription factor that has crucial roles in apoptosis, cell cycle arrest, cellular senescence, and DNA repair. Following exposure to a variety of stresses, p53 becomes post-translationally modified with concomitant increases in activity and stability. To better understand the role of acetylation of Lys-317 in mouse p53, the effect of ionizing radiation (IR) on the thymocytes of p53^{K317R} knock-in mice was studied at the global level. Using cleavable ICAT quantitative mass spectrometry, the effect of IR on protein levels in either the wild type or p53^{K317R} thymocytes was determined. We found 102 proteins to be significantly affected by IR in the wild type thymocytes, including several whose expression has been shown to be directly regulated by p53. When the effects of IR in the wild type and p53^{K317R} samples were compared, 46 proteins were found to be differently affected ($p < 0.05$). The p53^{K317R} mutation has widespread effects on specific protein levels following IR, including the levels of proteins involved in apoptosis, transcription, and translation. Pathway analysis of the differently regulated proteins suggests an increase in p53 activity in the p53^{K317R} thymocytes as well as a decrease in tumor necrosis factor α signaling. These results suggest that acetylation of Lys-317 modulates the functions of p53 and influences the cross-talk between the DNA damage response and other signaling pathways. *Molecular & Cellular Proteomics 7:716–727, 2008.*

p53 is one of the most important mammalian tumor suppressor proteins. It has been found to be mutated in approximately half of human cancers (1), and its functioning is frequently altered in many of the remainder (2). p53 is able to induce apoptosis, cell cycle arrest, DNA repair, and senescence in part through the activation or repression of numerous genes, including the cyclin kinase inhibitor *CDKN1A* (p21) and the proapoptotic proteins PUMA, NOXA, and PIDD (3).

The protein is able to bind DNA in a sequence-specific manner through its central DNA-binding domain, and it interacts with transcriptional co-activators and some co-repressors through N-terminal transactivation domains. The C-terminal portion of p53 contains nuclear localization signals, a tetramerization domain, and a regulatory domain that may repress the interaction of p53 with DNA (4).

p53 is maintained at low levels in unstressed cells but is stabilized and activated following DNA damage. This stabilization and activation coincides with extensive post-translational modification, including phosphorylation, acetylation, methylation, ubiquitylation, sumoylation, or neddylation at over 30 sites primarily in the N and C termini (5). These modifications may also regulate its interactions with other proteins (6). Acetylations of C-terminal lysine residues in p53 occur in response to various types of stress. The highly homologous and related histone acetyltransferases CBP[1] and p300 have been shown to acetylate six lysine residues: Lys-305, Lys-370, Lys-372, Lys-373, Lys-381, and Lys-382 (7, 8). Knock-in mice containing mutations of the homologous sites in mouse p53 exhibit moderately reduced p53 activity (9, 10). p300 and CBP-associated factor (PCAF) has been shown to specifically acetylate Lys-320 of human p53 following DNA damage (8, 11). PCAF forms part of SAGA-like chromatin remodeling complexes and functions as a transcriptional co-activator for several proteins, including the glucocorticoid receptor (12, 13). Initial studies of Lys-320 acetylation found that the modification increased binding of p53 to DNA, although the effects on *in vitro* transcription assays were small (8, 11). In contrast, a study of histone deacetylase inhibitor-induced apoptosis found that acetylation of p53 at Lys-320 correlated with increased expression of selected p53 target

[1] The abbreviations used are: CBP, cAMP-response element-binding protein (CREB)-binding protein; IR, ionizing radiation; GO, Gene Ontology; GR, glucocorticoid receptor; PCAF, p300 and CBP-associated factor; tpm, transcripts per million; EST, expressed sequence tag; PCNA, proliferating cell nuclear antigen; TNF, tumor necrosis factor; WT, wild type; ETFDH, electron-transferring-flavoprotein dehydrogenase; ILK, integrin-linked kinase; APIP, APAF1-interacting protein; CUGBP, CUG triplet repeat, RNA-binding protein; EGFR, epidermal growth factor receptor; PLAA, phospholipase A$_2$, activating protein; WARS, tryptophanyl-tRNA synthetase; NARS, asparaginyl-tRNA synthetase.

genes (14). In our previous characterization of mice containing knock-in missense mutation of the homologous Lys-317 residue of endogenous p53, we observed increased levels of apoptosis in thymocytes, epithelial cells of the small intestine, and cells of the retina after ionizing radiation (IR) in the p53[K317R] mice (15). Furthermore increased mRNA levels were observed for known p53 target genes after stress, including *p21*, *Mdm2*, *Puma*, *Pidd*, and *Noxa* (14, 15). These results suggested that acetylation of Lys-317 negatively regulates p53 apoptotic activity. Studies using a p53[K320Q] mutant, which mimics constitutive acetylation, support this conclusion (16). Recently Lys-320 of human p53 was shown to be subject to ubiquitylation by E4F1 or neddylation by FBXO11 (17, 18). The E4F1-induced ubiquitylation of p53 was shown to compete with PCAF-mediated acetylation and was associated with cell cycle arrest in UVC-irradiated U2OS cells (18).

In the present study, we used a cleavable ICAT quantitative proteomics method to further investigate the roles of the PCAF acetylation site of p53 by determining changes in protein levels following IR-induced DNA damage in thymocytes from wild type and p53[K317R] knock-in mice. The global proteomics study is complementary to our previous gene expression study (15) as regulation that operates at the level of translation or protein stability is not detected by analysis of mRNA levels. We found that the p53[K317R] mutation affects the response to IR of many proteins, including several involved in apoptosis, transcription, translation, and signal transduction. Our analysis suggests that acetylation of p53 at Lys-317 is important for modulating p53 cross-talk with other proteins and signaling pathways after IR.

EXPERIMENTAL PROCEDURES

Sample Preparation—The generation of knock-in mice containing the p53[K317R] mutation on both alleles of p53 was described previously (15). Four- to 6-week-old male mice, containing wild type p53 or p53[K317R], were left untreated or exposed to 5 grays of IR; after 8 h, the thymocytes from untreated and treated mice were harvested. The thymocyte samples used each represent the thymus of one mouse. Thymocytes were resuspended in lysis buffer (50 mM Tris, pH 7.5, 150 mM NaCl, 0.5% Nonidet P-40, 1 mM EDTA) and lysed by incubation at 4 °C for 30 min. Cellular debris were pelleted by centrifugation at 15,000 $\times$ g for 5 min at 4 °C. The total protein concentration in the supernatant was measured by BCA assay (Pierce). From each sample, an aliquot containing 500 μg of total protein was incubated with the appropriate cleavable ICAT reagent (Applied Biosystems) following the manufacturer's directions. Briefly each total protein sample was denatured and reduced by incubation in the supplied buffers for 10 min at 100 °C. Non-irradiated and irradiated samples were separately incubated with aliquots of the light and heavy reagents, respectively, for 2 h at 37 °C. The respective non-irradiated and irradiated samples from wild type or p53[K317R] mice were combined (total of 1 mg of protein) and digested with trypsin for 16 h at 37 °C. The labeled peptides were purified using cation exchange and avidin affinity cartridges. The biotin group on the tag was removed by acid cleavage, and the peptides were dried by vacuum evaporation using a Vacufuge (Eppendorf).

Mass Spectrometry—The dried peptides were resuspended in 100 μl of an aqueous solution containing 5% acetic acid and 5% acetonitrile. A 50-μl aliquot (equivalent to 500 μg of starting material) was loaded onto a 150 $\times$ 1.0-mm Polysulfoethyl A (5 μm, 200 Å) strong cation exchange column (PolyLC) and separated into 40 fractions using a gradient from 10 mM ammonium formate (pH 3), 10% acetonitrile to 0.5 M ammonium formate (pH 3), 10% acetonitrile over 40 min at 50 μl/min. Each fraction was diluted 1:1 with an aqueous buffer containing 2% acetonitrile, 1% formic acid, and 0.05% HFBA, and then half of the resulting solution was loaded onto a 0.1 $\times$ 150-mm Magic C18AQ reverse phase column (Michrom Bioresources, Inc.) in line after a nanotrap column using the Paradigm MS4 HPLC system (Michrom Bioresources, Inc.). Separation of the peptides was performed at 500 nl/min and was coupled to on-line analysis by tandem mass spectrometry using an LTQ ion trap mass spectrometer (ThermoElectron) equipped with a nanospray ion source (ThermoElectron). Elution of the peptides into the mass spectrometer was performed with a linear gradient from 95% mobile phase A (2% acetonitrile, 0.1% formic acid, 97.9% water) to 65% mobile phase B (10% water, 0.1% acetic acid, 89.9% acetonitrile) over 45 min followed by 95% mobile phase B over 5 min. The peptides were detected in positive ion mode using a data-dependent method in which the seven most abundant ions detected in an initial survey scan were selected for MS/MS analysis. Three technical replicate analyses were performed.

Data Analysis—The MS/MS spectra were searched against a mouse database containing 46,892 protein entries built from the National Center for Biotechnology non-redundant (NCBInr) database (downloaded May 2006) using TurboSEQUEST in BioWorks version 3.2 (ThermoElectron). The search parameters included: precursor mass tolerance, $\pm$ 2 amu; fragment mass tolerance, $\pm$ 1 amu; up to two missed trypsin cleavages; a static modification of +227.13 on cysteine for the light ICAT reagent; a variable modification of +9 on cysteine for the heavy ICAT reagent; and a variable modification for methionine oxidation. The search results were processed and analyzed using the Trans-Proteomic Pipeline (TPP) (Institute for Systems Biology). SEQUEST results were validated using the PeptideProphet software, which calculates a probability for each peptide identification (19). Quantitation was performed using the ASAPRatio software, which uses extracted ion chromatograms for quantitation, and the peptides were assigned to proteins using ProteinProphet (20, 21). Based in part on the peptide probability and the Sequest Xcorr score, a protein identification probability was calculated using Protein-Prophet; only protein identifications with a probability >0.9 were retained for further consideration. This cutoff results in a calculated false discovery rate of <1% as determined by ProteinProphet. All single peptide identifications were manually verified, and the quantifications were also manually checked. The ASAPRatio software uses a statistical method for identification of outliers and excludes them from quantification (20). Proteins for which constituent unique peptides exhibited significantly different ratios were excluded from further analysis. Peptides that matched to multiple members of a protein family were grouped as such by ProteinProphet and maintained as a protein family for analysis unless a peptide unique to a specific family member was observed; protein isoforms were maintained in the same way unless a peptide that uniquely identified the specific isoform was observed. Proteins that exist in the database under different names and/or accession numbers were grouped together for analysis. Proteins were classified as significantly IR-responsive if the p value calculated by the ASAPRatio software was less than 0.05. The significance of the differences in the IR-response ratios between the wild type and p53[K317R] samples was estimated using a Student's t test with a cutoff of $p < 0.05$. The identified proteins were analyzed using Ingenuity Pathways Analysis (Ingenuity® Systems). Functional analysis was performed using the FatiGO+ functional annotation software in the Babelomics suite (22, 23). The fraction of proteins identified out of those present in thymocytes was estimated from the set of curated mouse thymus ESTs. The thymus expression profile was extracted from

TABLE I

Peptides and proteins identified in the wild type and p53[K317R] ICAT experiments

	WT	K317R
Total unique peptides[a]	7103	7290
Average peptides per replicate	4130	4274
Total proteins identified[b]	1105	1080
Protein levels increased after IR[c]	66 (5.97%)	59 (5.46%)
Protein levels decreased after IR[c]	28 (2.53%)	36 (3.33%)

[a] As observed in three technical replicates.
[b] Proteins were required to have a probability >0.9 to be included.
[c] $p < 0.05$.

NCBI UniGene build 166 (August 21, 2007) (24) using a custom Perl script and collapsed to the level of gene symbols. The resulting collection contained 110,272 thymus ESTs associated with 12,372 gene symbols. The depth of proteome coverage was estimated by comparing transcript abundance for proteins identified in the wild type or p53[K317R] samples with transcript abundance for proteins not found.

Immunoblotting—To address biological variability, the immunoblotting samples were taken from different mice than those used for the mass spectrometry analysis. The thymocytes were lysed in co-IP buffer (10 mM Tris-HCl, pH 7.6, 140 mM NaCl, 5 mM EDTA, 0.5% Nonidet P-40) supplemented with protease inhibitors (Complete EDTA-free protease inhibitor mixture, Roche Applied Science). After separation by SDS-PAGE, the proteins were transferred to nitrocellulose membrane (Invitrogen). The immunoblots were probed with antibodies to ICAM-1 (M-19, Santa Cruz Biotechnology, Inc.), PCNA (PC10, Santa Cruz Biotechnology, Inc.), RPA-1 (Ab-1, Calbiochem), p21 (c-19, Santa Cruz Biotechnology, Inc.), and β-actin (AC-15, Sigma). Binding of the primary antibody was detected using IRDye 700DX-conjugated anti-mouse, anti-rabbit, or anti-goat IgG (Rockland) and an Odyssey Infrared Imaging System (LI-COR).

RESULTS

Proteomics Analysis of the Wild Type and p53[K317R] Thymocytes—To better understand the effects of PCAF acetylation of Lys-317 in mouse p53, wild type and p53[K317R] knock-in mice were exposed to IR. Only a small fraction of proteins identified in the wild type thymocytes exhibited a significant change in abundance after IR. Based on the MS/MS analysis of the paired, ICAT-labeled wild type samples, a total of 7103 unique peptides were identified in three technical replicates, with an average of 4130 peptides (2367 unique peptides) identified per replicate run (Table I). The identified peptides resulted in the identification and relative quantification of 1105 proteins with an expected false discovery rate of less than 1%. Of the proteins identified and quantified, 69% were observed in more than one replicate and 68% were identified by two or more unique peptides. The latter proportion is consistent with other studies using quantification based on residue-specific labeling (25). Of the proteins quantified, the relative amounts of 102 proteins (9.2%) were significantly changed by exposure to IR ($p < 0.05$). The fraction of affected proteins is similar to the proportion of genes found to be significantly affected by IR in gene expression studies of thymocytes (15).

Similarly in the p53[K317R] mutant thymocytes, a small fraction of proteins identified exhibited a significant change in abun-
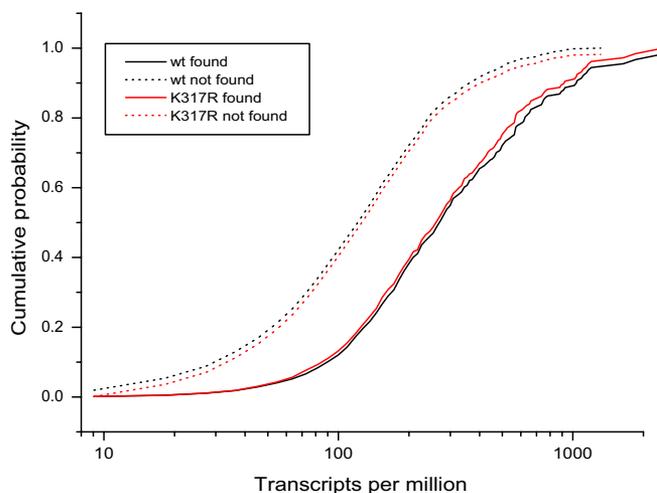

FIG. 1. **Cumulative probability distributions for identified and not-identified proteins in the wild type and p53[K317R] experiments.** The NCBI UniGene thymus expression profile was used to estimate transcript abundance. Identified proteins were associated with transcripts through their associated gene symbols. The cumulative probability distributions for proteins that were identified (*solid*) or not identified (*dotted*) in the wild type (*black*) and p53[K317R] (*red*) experiments are shown.

dance after IR. The MS/MS analysis of the paired p53[K317R] samples resulted in the identification of a total of 7290 unique peptides in three technical replicates, with an average identification of 4274 peptides (2430 unique peptides) per replicate run (Table I). The identified peptides resulted in the identification and relative quantification of 1080 proteins, with 68% being identified by two or more unique peptides and 62% observed in more than one replicate run (Table I). Of the proteins quantified, 105 (9.7%) were significantly affected by IR ($p < 0.05$) (Table I and supplemental Table 1). Overall the numbers of proteins identified and significantly affected by IR are similar in the wild type and p53[K317R] analyses.

To estimate the depth of proteome coverage, the NCBI *Mus musculus* thymus expression profile was used as a measure of transcript abundance (24). Mouse thymus transcript abundance, expressed as transcripts per million (tpm), was used as a proxy for protein abundance in thymocytes. As shown in Fig. 1, the cumulative probability distribution functions for proteins found or not found in the MS/MS analysis of the wild type and p53[K317R] samples display a similar dependence on transcript abundance. The mean abundance of the not-found proteins was 73 tpm for either experiment, whereas the mean abundance of the found proteins was 185 tpm for the wild type samples and 178 for the p53[K317R] samples. The mean transcript abundance for the found proteins is ~2.5-fold larger than the mean transcript abundance for the not-found proteins. We note that as the UniGene EST expression profile is based upon whole thymus, differences in gene expression patterns between thymocytes and thymic stroma (26) will contribute to the separation between the mean transcript abundance for identified and not-found thymocyte proteins.

A

Biological Process - Level 6

Percent of Proteins in List

B

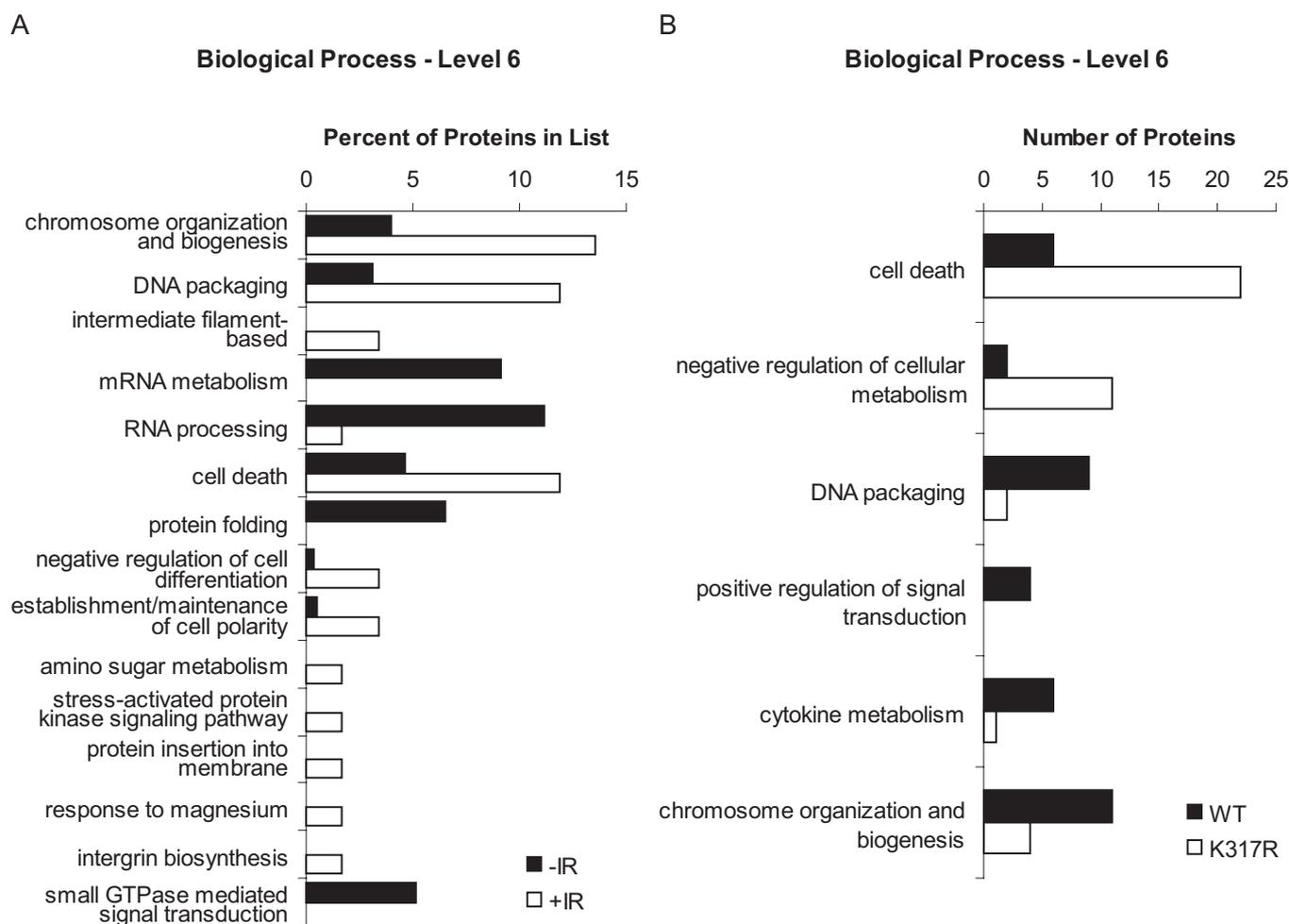**Biological Process - Level 6**

Number of Proteins

FIG. 2. **Gene Ontology biological process classification of proteins observed.** The categories of biological process, level 6, that differed significantly ($p < 0.1$) are shown. *A*, proteins significantly affected by IR in the wild type thymocytes with those responsive to IR shown in *white* and those unresponsive to IR shown in *black*. *B*, processes that differ significantly between the wild type and p53^K317R data sets with proteins from the wild type shown in *black* and proteins from the p53^K317R data set shown in *white*.

The small difference between the means suggests that the identification of proteins by tandem mass spectrometry in our system is not restricted to the most abundant proteins (19). In particular, the curves for the found proteins and not-found proteins are very similar, indicating little bias towards detection of more prevalent proteins. If only more abundant proteins were detected in our system, the cumulative probability curves for found and not-found proteins would be farther apart for low transcript abundance and closer together for high transcript abundance. Moreover, the similarity of the distributions for the wild type and p53^K317R experiments indicates a high degree of reproducibility in the experiments.

Functional annotations of the proteins identified in the two experiments were compared using the FatiGO+ algorithm (22, 23). Proteins that had been identified and quantified in the wild type or p53^K317R experiments were classified by their Gene Ontology (GO) molecular function, level 3 (supplemental Fig. 1A), and biological process, level 6 (supplemental Fig. 1B), categories. Approximately 800 proteins from each list

were associated with a functional annotation. The molecular function categories of annotated proteins in the two data sets are quite similar with none of the functions differing significantly ($p < 0.1$) between the two (supplemental Fig. 1A). This supports the suggestion that similar types of proteins were identified in both experiments and that there was not a bias in one sample or the other. As discussed in greater detail below, the representation of the identified proteins in several GO biological process categories differed significantly between wild type and p53^K317R thymocytes.

IR-induced Changes in the Abundance of Specific Proteins in Wild Type Thymocytes—To the best of our knowledge, this study represents the first analysis of IR-induced changes in the thymocyte proteome. As indicated above, ~10% of the identified proteins exhibited a significant ($p < 0.05$) change in abundance after IR. In comparison with proteins unaffected by IR, proteins involved in cell death were significantly over-represented ($p < 0.1$) among the proteins significantly affected by IR (Fig. 2A). Proteins involved in chromosome or-

TABLE II

Proteins identified to be significantly (p < 0.05) affected by IR in the wild type thymocyte samples

NCBI accession no.	Description	Gene symbol	Ratio (−IR/+IR)	S.D.	Pep[a]
NP_001005331	Eukaryotic translation initiation factor 4, γ1	Eif4g1	0.05	0.01	1
NP_598445	MOCO sulfurase C-terminal domain-containing 2	Mosc2	0.05	0.01	2
NP_080750	SGT1, suppressor of G2 allele of SKP1	Sugt1	0.05	0.01	2
NP_067498	HECT, UBA, and WWE domain-containing 1	Huwe1	0.10	0.01	1
NP_001074525	Exportin, tRNA	Xpot	0.10	0.01	2
NP_038946	Ubiquitin-specific peptidase 25	Usp25	0.11	0.02	1
NP_598924	Muscleblind-like 3	Mbnl3	0.12	0.02	1
NP_033140	S100 calcium-binding protein A9 (calgranulin B)	S100a9	0.13	0.04	6
NP_035831	Vimentin	Vim	0.14	0.03	3
NP_038678	S100 calcium-binding protein A8 (calgranulin A)	S100a8	0.14	0.02	4
NP_033980	CD3 antigen, γ polypeptide	Cd3g	0.16	0.03	1
NP_663521	General transcription factor IIB	Gtf2b	0.17	0.02	2
NP_034692	Integrin-linked kinase	Ilk	0.18	0.01	1
NP_113581	Actin-like 6B	Actl6b	0.18	0.03	2
NP_080858	Putative NF-κ B-activating protein 373	Gpr177	0.19	0.03	2
NP_032548	Lactotransferrin	Ltf	0.19	0.12	11
NP_032246	Hemoglobin, β adult major chain	Hbb-b1	0.19	0.03	6
NP_058063	Progesterone receptor membrane component	Pgrmc1	0.21	0.01	2
NP_062414, NP_034114	Cathepsin 8, cathepsin L preproprotein	Cts8, Ctsl	0.21	0.02	3
NP_034022	Chitinase 3-like 3	Chi3l3	0.21	0.13	8
NP_064432	Trf-proximal protein homolog	Trfp	0.22	0.03	1
NP_031960	Glutamyl aminopeptidase	Enpep	0.22	0.03	1
NP_001074599	Oxoglutarate dehydrogenase-like	Ogdhl	0.22	0.02	2
NP_033784	Albumin 1	Alb	0.23	0.13	19
NP_059066	Haptoglobin	Hp	0.23	0.04	1
NP_067448	Aldo-keto reductase family 1, member A4 (aldehyde reductase)	Akr1a4	0.24	0.06	2
NP_032199	Nuclear receptor subfamily 3, group C, member 1	Nr3c1	0.25	0.04	2
NP_031650	Chromobox homolog 3	Cbx3	0.25	0.06	2
NP_038499	Annexin A4	Anxa4	0.26	0.02	5
NP_937812	Glucocorticoid modulatory element-binding protein 2	Gmeb2	0.26	0.02	2
NP_062513, NP_075679	Apoptotic chromatin condensation inducer 1	Acin1	0.26	0.01	2
NP_032255	Histone deacetylase 2	Hdac2	0.27	0.04	2
NP_067620	Nicastrin	Ncstn	0.27	0.02	1
NP_035908	Coronin, actin-binding protein 1B	Coro1b	0.27	0.06	2
NP_033941	Caspase 6	Casp6	0.28	0.08	3
NP_082568	Protein phosphatase methylesterase 1	Ppme1	0.28	0.03	2
NP_038853	Lymphocyte antigen 75	Ly75	0.28	0.06	4
NP_996988	Response to metastatic cancers 1	H2-Ab1	0.28	0.10	12
NP_058020	S100 calcium-binding protein A11 (calizzarin)	S100a11	0.28	0.03	5
NP_444389	Mitochondrial ribosomal protein L3	Mrpl3	0.29	0.05	1
NP_032720	Neutrophilic granule protein	Ngp	0.29	0.06	4
NP_031652	Chromobox homolog 5 (*Drosophila* HP1a)	Cbx5	0.30	0.09	4
NP_036153, NP_036154, NP_033384, NP_937811	Regulatory subunit B56, protein phosphatase 2A[b]		0.30	0.04	2
NP_780519	Androgen-induced proliferation inhibitor	Pds5b	0.30	0.06	4
NP_034764	Fatty acid-binding protein 5	Fabp5	0.30	0.05	4
NP_062708	*N*-Acylsphingosine amidohydrolase (acid ceramidase) 1	Asah1	0.31	0.03	2
NP_034954	Myeloperoxidase	Mpo	0.32	0.05	7
XP_194337	Multiple EGF-like domains 8	Megf8	0.32	0.05	1
NP_035753	Topoisomerase (DNA) II α	Top2a	0.33	0.04	3
NP_444354	SWI/SNF-related, matrix-associated, actin-dependent regulator of chromatin, subfamily a, member 5	Smarca5	0.33	0.05	2
NP_034623	Intercellular adhesion molecule	Icam1	0.33	0.04	2
NP_056594	Neutrophil elastase	Ela2	0.33	0.02	2
NP_035840	Tryptophanyl-tRNA synthetase	Wars	0.34	0.04	4
NP_081212	Oxidase assembly 1-like	Oxa1l	0.34	0.03	1
NP_062709	APAF1-interacting protein	Apip	0.34	0.02	2

TABLE II—*continued*

NCBI accession no.	Description	Gene symbol	Ratio (−IR/+IR)	S.D.	Pep[a]
NP_033364	Acetyl-coenzyme A acetyltransferase 2	Acat2	0.34	0.07	2
NP_034960	MutS homolog 6	Msh6	0.35	0.04	3
NP_036151	Peroxiredoxin 5 precursor	Prdx5	0.35	0.07	2
NP_064337	Transmembrane protein 4	Tmem4	0.36	0.07	4
NP_892035	Structure-specific recognition protein 1	Ssrp1	0.37	0.04	2
NP_058622	Squamous cell carcinoma antigen recognized by T-cells 3	Sart3	0.37	0.04	1
NP_766283	Phospholipase A2, activating protein	Plaa	0.37	0.05	2
NP_033357	Transcription factor 7, T-cell-specific	Tcf7	0.38	0.05	2
NP_038579	Hydroxymethylbilane synthase	Hmbs	0.38	0.06	1
NP_598738	Transferrin	Trf	0.39	0.06	2
NP_080070	Electron transferring flavoprotein dehydrogenase	Etfdh	0.40	0.08	3
NP_775621	RCC1 domain-containing 1	Rccd1	0.40	0.03	1
NP_036167	Vesicle amine transport protein 1 homolog (*Torpedo californica*)	Vat1	0.41	0.04	3
NP_082442	Hypothetical protein LOC72244	1600014C10Rik	0.41	0.16	3
NP_034851	Lamin B1	Lmnb1	0.45	0.19	3
NP_034793	Keratin complex 1, acidic, gene 17	Krt17	0.45	0.13	3
NP_080784	TNF receptor-associated protein 1	Trap1	1.49	0.01	2
NP_067497	Ubiquitin-specific protease 14	Usp14	1.78	0.02	2
NP_114084	SWI/SNF related, matrix-associated, actin-dependent regulator of chromatin, subfamily d, member 2	Smarcd2	1.87	0.06	3
NP_035407	Ring finger protein 2	Rnf2	2.39	0.24	1
NP_080120	Cysteine- and histidine-rich domain (CHORD)-containing, zinc-binding protein 1	Chordc1	2.59	0.32	3
NP_077180	Ribosomal protein L24	Rpl24	2.60	0.50	7
NP_033035	RAD21 homolog	Rad21	2.64	0.29	5
NP_034745	Kinesin family member 11	Kif11	2.69	0.09	2
NP_036105	Ribosomal protein L27a	Rpl27a	2.70	0.53	2
NP_683747,NP_080225, NP_033123,NP_035429	Ribosomal protein S6 kinase[c]		2.97	0.64	2
NP_666054	3-Hydroxy-3-methylglutaryl-coenzyme A synthase 1	Hmgcs1	3.05	0.39	2
NP_150289	Cyclic AMP-regulated phosphoprotein, 21 isoform 2	Arpp21	3.08	0.42	1
NP_038484	Actinin α 3	Actn3	3.12	0.51	2
NP_766607	6-Phosphofructo-2-kinase/fructose-2,6-biphosphatase 4	Pfkfb4	3.29	0.48	2
NP_033785	Activated leukocyte cell adhesion molecule	Alcam	3.37	0.52	2
NP_081626	Asparaginyl-tRNA synthetase	Nars	3.46	0.35	1
NP_033109	Ribosomal protein L30	Rpl30	3.52	0.44	4
NP_033120	Ribosomal protein S4, X-linked	Rps4x	3.96	0.70	8
NP_033240	Spermine synthase	Sms	3.96	0.44	2
NP_062648	Protein phosphatase 4, catalytic subunit	Ppp4c	4.07	0.68	1
NP_796307	SEC6-like 1	Exoc3	4.17	0.65	1
NP_082253	RIKEN cDNA 2310001A20	2310001A20Rik	4.64	0.45	3
NP_780314	Aquaporin 11	Aqp11	5.78	0.68	1
NP_038573	Hemopoietic cell phosphatase	Ptpn6	6.55	2.00	4
NP_081291	Ribosomal protein S27	Rps27	7.26	1.48	2
NP_569054	Toll-like receptor 3	Tlr3	8.91	2.64	2
NP_075029	Ribosomal protein L23	Rpl23	9.76	1.82	2
NP_112442	Heat shock protein 8	Hspa8	14.42	3.27	2

[a] For proteins identified by a single peptide, the sequence, precursor mass, charge, and Xcorr score for the peptide identified is provided in supplemental Table 2; MS/MS spectra for those peptides are provided in supplemental Fig. 3.
[b] Unable to discriminate the γ, ϵ, δ, and β isoforms.
[c] Unable to discriminate polypeptides 1, 2, 3, and 6.

ganization and biogenesis, DNA packaging, intermediate filament-based processes, negative regulation of cell differentiation, and stress-activated protein kinase signaling were also overrepresented among proteins affected by IR (Fig. 2*A*). In contrast, proteins involved in mRNA metabolic processes, RNA processing, protein folding, and small GTPase signal transduction were underrepresented among proteins affected by IR compared with proteins not affected by IR.

The relative levels of several proteins involved in transcription were affected by IR. For example, ring finger protein 2, a negative regulator of transcription, decreased in protein level after IR (Table II). Interestingly, however, the levels of several
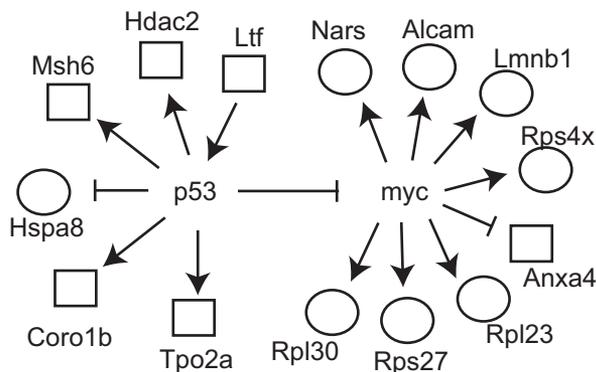
FIG. 3. **Schematic diagram showing functional links between p53 and proteins that exhibit IR-induced changes in protein levels in WT thymocytes ($p < 0.05$).** Proteins represented by *squares* increased after IR, and those represented by *circles* decreased after IR.

FIG. 4. **Immunoblots of selected proteins from untreated or irradiated wild type and p53^K317R thymocytes.** PCNA, RPA-1, ICAM-1, and actin were identified and quantified by mass spectrometry. p21, a known p53 target, was not.

ribosomal proteins decreased following IR (Table II), suggesting that IR has an effect on translation.

Six proteins that play a positive role in apoptosis were identified, with a range of increased and decreased levels after IR. The levels of ACIN1, CASP6, CDG3, and MSH6 increased, whereas the amounts of ACTN3 and PTPN6 decreased (Table II). Similarly five proteins that have a positive role in cell proliferation exhibited a range of changes; the levels of ENPEP and ILK increased after IR, whereas those of PPP4C, RAD21, and RPS4X decreased. The levels of four negative regulators of apoptosis, ALB1, ANXA4, APIP, and MPO, decreased after IR, whereas the levels of PDS5B, S100A11, and WARS, which are negative regulators of cell proliferation, increased (Table II).

Analysis of the proteins significantly affected by IR in the wild type thymocytes revealed two main networks of functional relationships. The first network centered on p53 (Fig. 3), known to be essential for IR-induced apoptosis in thymocytes (27, 28). Some changes in protein levels after IR can be directly linked to p53 transcription-modulating activity, including HDAC2, which is induced by p53, and HSPA8, which is repressed (29). A second network centered on c-*myc* (Fig. 3), which has been shown to be repressed by p53 (30). Proteins such as RPS4X and NARS, that are up-regulated by *myc*, decreased after IR, whereas proteins that are down-regulated by MYC, such as annexin A4, increased after IR (31–33). This pattern suggests that MYC activity is repressed after IR, likely by p53.

Changes in Protein Levels in the p53^K317R Thymocytes after IR Reveal Wide Reaching Roles of p53—As mentioned above, the representation of identified proteins in several GO biological process (level 6) categories differed between the wild type and p53^K317R experiments (Fig. 2B). A significantly ($p < 0.1$) greater number of proteins involved in cell death were identified in the p53^K317R experiment than in the wild type, as were proteins involved in the negative regulation of cellular metabolism (Fig. 4 and supplemental Fig. 1B). Fewer proteins that function in DNA packaging, positive regulation of signal trans-
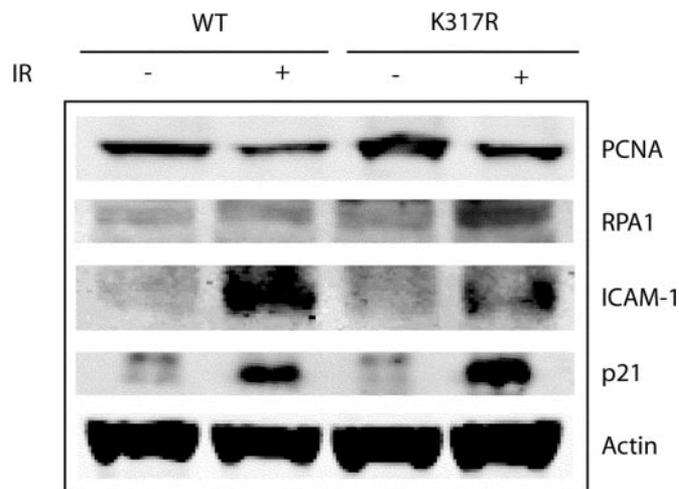
duction, cytokine metabolism, and chromosome organization and biogenesis were identified in the p53^K317R experiment. The increased number of cell death-associated proteins in the p53^K317R experiment is especially interesting given the increased level of apoptosis previously reported in the p53^K317R thymocytes (15).

When the wild type and p53^K317R data sets were compared, 786 proteins were common to both. Of the common proteins, 46 were found to be differently affected by IR in wild type and p53^K317R thymocytes (Table III). Among them are 22 proteins for which the wild type IR response was lost and 15 proteins that showed an IR response in the p53^K317R thymocytes but not in the wild type. Additionally one protein, PPP4C, decreased after IR in the wild type but increased after IR in the p53^K317R sample.

Several proteins with roles in apoptosis were identified to be affected differently after IR. PPP4C, which decreased in abundance after IR in the wild type thymocytes but increased in the mutant, has been shown to be proapoptotic in thymocytes (34). It is thought that TRAP1 suppression results in an increase in formation of reactive oxygen species that enhances apoptotic signaling, and it has been found to decrease in a time-dependent manner during apoptosis (35, 36). TRAP1 decreased 1.5 times in the wild type and 4 times in the mutant (Table III). ACIN1, CASP6, and RAD21 are all cleaved during apoptosis, and this cleavage is important for apoptotic signaling (37–39). Interestingly an ACIN1 peptide that spans the caspase cleavage site was observed in both the wild type and p53^K317R experiments (supplemental Fig. 2). Thus, quantification of this peptide, which increased after IR in the wild type but did not change significantly after IR in the mutant, represents the uncleaved, inactive form of the protein. It is likely then that the unchanged relative level of ACIN1 after IR in the p53^K317R sample is due to increased processing of ACIN1,

TABLE III

Proteins with a significant (p < 0.05) change in protein level after IR between the wild type and p53^{K317R} thymocytes

Accession number	Description	Gene symbol	WT (−IR/+IR)	WT S.D.	K317R (−IR/+IR)	K317R S.D.	p value, WT vs. K317R
NP_075631	Actin-related protein 2/3 complex, subunit 1B	Arpc1b	1.09	0.11	0.32	0.04	0.011
NP_038484	Actinin α3	Actn3	3.12	0.51	1.22	0.25	0.000
NP_077175	Anaphase-promoting complex subunit 4	Anapc4	0.51	0.06	0.11	0.02	0.012
NP_780519	Androgen-induced proliferation inhibitor	Pds5b	0.30	0.06	0.96	0.15	0.029
NP_062513 NP_075679	Apoptotic chromatin condensation inducer 1	Acin1	0.26	0.01	0.75	0.05	0.003
NP_033941	Caspase 6	Casp6	0.28	0.08	1.35	0.23	0.013
NP_062414 NP_034114	Cathepsin 8, cathepsin L preproprotein[a]		0.21	0.02	0.49	0.10	0.010
NP_033980	CD3 antigen, γ polypeptide	Cd3g	0.16	0.03	0.55	0.09	0.019
NP_033970	Chaperonin subunit 8 (θ)	Cct8	0.72	0.31	2.20	0.45	0.009
NP_035908	Coronin, actin-binding protein 1B	Coro1b	0.27	0.36	0.77	0.09	0.008
NP_034290	CUG triplet repeat, RNA-binding protein 2	Cugbp2	0.92	0.18	5.36	0.67	0.000
NP_080120	Cysteine- and histidine-rich domain (CHORD)-containing, zinc-binding protein 1	Chordc1	2.59	0.32	0.92	0.29	0.038
NP_444341	Eosinophil-associated, ribonuclease A family, member 6	Ear6	0.99	0.16	2.37	0.39	0.018
NP_075643	ETHE1 protein	Ethe1	1.00	0.15	0.51	0.12	0.033
NP_034764	Fatty acid-binding protein 5, epidermal	Fabp5	0.30	0.05	0.92	0.03	0.004
NP_031960	Glutamyl aminopeptidase	Enpep	0.22	0.03	0.07	0.00	0.018
NP_038573	Hemopoietic cell phosphatase	Ptpn6	6.55	2.00	0.78	0.15	0.000
NP_849209	Hydroxyacyl-coenzyme A dehydrogenase/3-ketoacyl-coenzyme A thiolase/enoyl-coenzyme A hydratase (trifunctional protein), α subunit	Hadha	1.18	0.15	0.11	0.02	0.002
NP_034623	Intercellular adhesion molecule	Icam1	0.33	0.04	1.16	0.10	0.000
NP_075552	Interferon γ-inducible protein 30	Ifi30	0.65	0.07	0.30	0.06	0.021
NP_056598	Interferon α-inducible protein	Isg15	1.64	0.24	0.48	0.08	0.023
NP_032548	Lactotransferrin	Ltf	0.19	0.12	0.42	0.32	0.028
NP_080104	Lectin, mannose-binding 2	Lman2	0.80	0.13	6.01	1.30	0.030
NP_032720	Neutrophilic granule protein	Ngp	0.29	0.06	0.52	0.12	0.008
NP_032199	Nuclear receptor subfamily 3, group C, member 1	Nr3c1	0.25	0.04	0.08	0.02	0.031
NP_036151	Peroxiredoxin 5 precursor	Prdx5	0.35	0.07	0.70	0.09	0.008
NP_766283	Phospholipase A2, activating protein	Plaa	0.37	0.05	0.84	0.14	0.023
NP_079826	Proteasome, 26 S, non-ATPase regulatory subunit 6	Psmd6	0.48	0.08	0.26	0.07	0.049
NP_062648	Protein phosphatase 4, catalytic subunit	Ppp4c	4.07	0.68	0.10	0.03	0.014
NP_033035	RAD21 homolog	Rad21	2.64	0.29	1.30	0.31	0.016
	Regulatory subunit B56, protein phosphatase 2A[b]		0.30	0.04	1.91	0.25	0.031
NP_080929	Replication protein A1	Rpa1	0.74	0.03	0.50	0.05	0.026
NP_033109	Ribosomal protein L30	Rpl30	3.52	0.44	1.46	0.21	0.001
NP_079863	Ribosomal protein S21	Rps21	1.10	0.13	0.39	0.06	0.018
NP_081291	Ribosomal protein S27	Rps27	7.26	1.48	2.00	0.63	0.010
NP_033120	Ribosomal protein S4, X isoform	Rps4x	3.65	0.50	1.22	0.32	0.000
NP_082253	RIKEN cDNA 2310001A20	2310001A20Rik	4.64	0.45	1.05	0.09	0.002
NP_080750	SGT1, suppressor of G2 allele of SKP1	Sugt1	0.05	0.01	1.09	0.37	0.009
NP_080451	Splicing factor 3a, subunit 1	Sf3a1	1.00	0.12	2.64	0.43	0.035
NP_058622	Squamous cell carcinoma antigen recognized by T-cells 3	Sart3	0.37	0.04	1.07	0.09	0.007
NP_613051	SR-related CTD-associated factor 6	Cherp	0.73	0.13	0.27	0.04	0.039
NP_892035	Structure-specific recognition protein 1	Ssrp1	0.37	0.04	0.62	0.10	0.033
NP_444354	SWI/SNF-related, matrix-associated, actin-dependent regulator of chromatin, subfamily a, member 5	Smarca5	0.33	0.05	0.93	0.18	0.003
NP_080784	TNF receptor-associated protein 1	Trap1	1.49	0.01	4.41	0.28	0.012
NP_035840	Tryptophanyl-tRNA synthetase	Wars	0.34	0.04	0.48	0.06	0.047
NP_067497	Ubiquitin-specific protease 14 isoform 1	Usp14	1.78	0.02	0.93	0.11	0.009

[a] Unable to discriminate the two proteins.
[b] Unable to discriminate the γ, ε, δ, and β isoforms.

consistent with the observed increased level of apoptosis in the mutant thymocytes.

Nine proteins whose levels were significantly affected by IR are known to be involved in transcription and/or translation. One transcription factor, glucocorticoid receptor (GR), increased 4-fold in the wild type and 12.5-fold in the mutant. Interestingly GR is known to be important for apoptosis during T-cell selection (40). SSRP1 is part of the FACT complex that interacts with histones H2A and H2B to disassemble nucleosomes for transcription (43). SSRP1 increased 2.7-fold after IR in the wild type but did not increase significantly in the mutant. Interestingly SSRP1 has been shown to be degraded during apoptosis; it is possible that the lower relative amount of this protein in the mutant *versus* wild type thymocytes is related to increased apoptosis as a result of the mutation (44). These results suggest that important differences occur in the regulation of transcription between the wild type and p53^{K317R} thymocytes.

Two spliceosome proteins identified, CUGBP and SF3A1, showed a significant decrease after IR in the mutant sample but not in the wild type (Table III). In addition, SART3, which is important for recycling of the spliceosome, lost the increase in protein level in the mutant that was observed after IR in the wild type (45). Three ribosomal proteins showed an increase in protein level in the mutant relative to the wild type. RPL30 and RPS27 showed at least a 2.5-fold decrease after IR in the wild type but had no significant change after IR in the p53^{K317R} sample (Table III). RPS21 was not affected by IR in the wild type but increased 2.5 times after IR in the mutant (Table III). Together these differences suggest a change in the regulation of translation in the mutant thymocytes.

Validation—The cleavable ICAT method allows the relative quantification of hundreds of proteins in one experiment. We chose a few proteins to validate by Western blotting. Immunoblots with antibodies against RPA-1, PCNA, and actin showed changes after IR similar to those that were observed by mass spectrometry in the wild type and p53^{K317R} samples (Fig. 4). For example, by Western blotting, PCNA decreased 0.6 times after IR in the wild type and 0.7 times in the mutant; the mass spectrometry-based quantification showed a decrease of 0.6 times in the wild type and 0.8 times in the mutant. The ICAM-1 blot showed increased expression after IR in the wild type and a smaller increase in the p53^{K317R} sample; this is in qualitative but not quantitative agreement with the mass spectrometry result. Furthermore the immunoblot of p21, a known p53 target gene that was not detected by mass spectrometry, showed a greater increase in protein level after IR in the mutant relative to the wild type (Fig. 4): the protein level increased 2.2-fold after IR in the wild type and 6.7-fold in the mutant. This result confirms that p53 is more active after IR in the mutant thymocytes than in the wild type thymocytes.

DISCUSSION

Previous studies have shown that mutation of mouse p53 at Lys-317 or human p53 at Lys-320 results in increased apoptosis (15, 16). These studies have found that mutation of this site to arginine results in p53 that is more active as a transcription factor, with a greater induction of some target genes after IR in the mutant than in the wild type. Because regulation can occur post-transcriptionally as well as through transcriptional control, we used a quantitative proteomics method to investigate the effects of the p53^{K317R} mutation on IR-induced changes in protein levels in mouse thymocytes. To the best of our knowledge, this study represents the first proteomics analysis of the IR response in thymocytes. We identified over 1000 proteins with ~10% of them exhibiting significant IR-induced changes in abundance (Table I). This quantitative analysis identified lower abundance proteins as well as higher abundance proteins, demonstrating that the cysteine-based ICAT labeling and ion trap MS/MS method provided a good depth of coverage. The identified proteins are involved in a range of molecular functions and biological processes (supplemental Fig. 1), indicating that a wide representation of proteins was identified.

Of the proteins that were quantified in both the wild type and p53^{K317R} samples, 6% had significantly ($p < 0.05$) different relative abundances after IR (Table III). Surprisingly few p53 target gene products that are known to be regulated by IR in thymocytes (15) were identified in these experiments. Detection of these proteins may be difficult because they are present at low levels or because of other intrinsic characteristics. For example, PUMA does not have any cysteine-containing tryptic peptides of a suitable size for analysis and consequently could not be observed by the methodology used here. Interestingly BAX (Bcl2-associated X protein), a proapoptotic p53 target protein, was identified in both the wild type and p53^{K317R} experiments but did not exhibit a significant change in protein level following IR in either sample (data not shown).

Pathway analysis of the proteins for which the IR-induced changes in protein level differed significantly between the wild type and p53^{K317R} samples revealed two main networks. The first network is related to cell death and includes links between p53 and several growth factor receptor proteins (Fig. 5A). Notably, CORO1B protein levels increased after IR in wild type thymocytes but remained essentially unchanged in mutant thymocytes. The loss of increase in protein level is consistent with a recent study showing CORO1B to be induced by p53 in neuronal outgrowth only when Lys-320 was acetylated (46). Furthermore, p53 induces expression of EGFR (47), and EGFR regulates the expression of ACTN3 and USP14, two proteins that increased in expression in the mutant but not significantly in the wild type (48). p53 represses IGFR1R activity and expression (49); this in turn represses RPL24 expression (50); increased p53 activity could then lead to
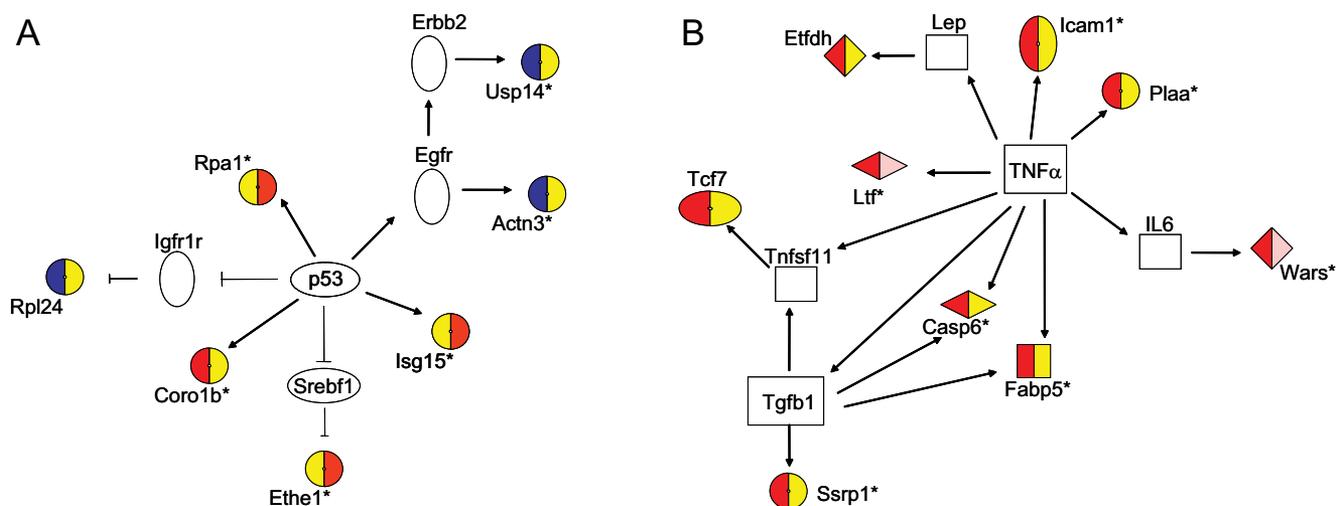
FIG. 5. **Schematic diagrams linking groups of proteins for which the IR response differs significantly between WT and p53^K317R thymocytes.** *A*, p53 and group 1; *B*, TNFα and group 2. Linked proteins that were not identified and quantified by mass spectrometry are indicated by *unfilled symbols*. The *colors* on the *left* and *right halves* of the *filled symbols* represent the wild type IR effect and the p53^K317R IR effect, respectively, on protein levels: *blue*, decreased; *yellow*, unchanged; and *red*, increased. Gene symbols for quantified proteins that were significantly different at $p < 0.05$ are marked with an *asterisk*; others were significantly different at $p < 0.1$.

increased RPL24 levels as observed in the mutant thymocytes relative to the wild type thymocytes.

The second network comprises proteins linked to TNFα (Fig. 5B). The pattern of changes in protein levels suggests that TNFα activity was not affected by IR in the p53^K317R samples, whereas it increased after IR in the wild type samples. Specifically TNFα has been shown to up-regulate PLAA and CASP6 (51, 52), both of which increased after IR in the wild type but not in the mutant. Decreased TNFα activity in p53^K317R thymocytes is also consistent with the observed lack of change in WARS, TCF7, and ETFDH protein levels after IR; all of these proteins are indirectly regulated by TNFα (53–58). Finally TNFα has been shown to induce the expression of TGFβ1 (59), which has been shown to increase the expression of FABP5 and SSRP1 (60, 61), two additional proteins that exhibit the same pattern. Thus, the proteins affected differently by IR in wild type compared with mutant thymocytes suggest a change in p53 activity and a decrease in TNFα signaling.

The interactions between the TNFα and p53 signaling pathways are complex and are affected by both the type of cell and type of stress. Although as a proinflammatory cytokine TNFα often opposes p53 activity (62), it has been shown to induce p53 and increase p53-dependent apoptosis (63). Conversely p53 may increase TNFα-dependent apoptosis through induction of a proapoptotic factor (64) or indirectly regulate TNFα signaling through the GR. We found that GR protein levels increased 4-fold after IR in wild type thymocytes and 12.5-fold in p53^K317R thymocytes. GR has been shown to be required for glucocorticoid-mediated apoptosis after DNA damage in thymocytes, and mutational studies have suggested that an increase in GR levels, as observed here, results

in an increase in apoptosis in thymocytes (40, 65). GR has been shown to interfere with NF-κB activity and TNFα signaling, possibly by preventing the recruitment of essential cofactors (66). Furthermore GR is known to decrease ICAM-1 expression through repression of NF-κB activation of the gene (67). GR-mediated apoptosis is effected through the same pathway as p53-mediated apoptosis, involving the Bcl2 family members (40).

Previous research has suggested cross-talk between the p53 and GR pathways (68, 69). Interestingly, the interaction between the two proteins is mediated through the part of p53 that includes Lys-320. p53 is acetylated at Lys-320 by PCAF, a cofactor that is also required by GR for its activity. A study of p53^K320Q, which mimics constitutive acetylation, demonstrated that PCAF binds more readily to acetylated p53 than non-acetylated p53 (16). Lys-320 acetylation may allow p53 to sequester PCAF, thus modulating the activity of other transcription factors. As mentioned above, a similar mechanism has been proposed for GR-mediated interference with other transcription factors (65).

Additionally, Lys-320 lies within one of the nuclear localization signals of p53 and has been shown to be required for proper localization of the protein (41). p53^K320Q was found to localize predominantly in the cytoplasm, whereas p53^K320R localized primarily in the nucleus (16, 42). Acetylation at Lys-320 may modify the localization of p53 and, in turn, affect the localization of proteins that are sequestered in the cytoplasm by p53. For example, p53 has been shown to bind GR through its core domain and nuclear localization signal, and this binding sequesters both p53 and GR in the cytoplasm (68, 69). It is possible then that the increased nuclear localization of p53^K317R allows the movement of GR into the nucleus, in-

creasing glucocorticoid-mediated apoptosis at the same time as p53-dependent apoptosis.

In conclusion, we found several proteins to be regulated differently after IR in wild type and p53^{K317R} thymocytes. Our findings suggest a role of Lys-320 acetylation in modulating the interactions of p53 that may affect cross-talk between different transcriptional pathways. Further experiments are required to understand the full extent of the pathways affected by this modification.

REFERENCES

1. Hollstein, M., Sidransky, D., Vogelstein, B., and Harris, C. C. (1991) p53 mutations in human cancers. *Science* **253,** 49–53
2. Woods, D. B., and Vousden, K. H. (2001) Regulation of p53 function. *Exp. Cell Res.* **264,** 56–66
3. Oren, M. (2003) Decision making by p53: life, death and cancer. *Cell Death Differ.* **10,** 431–432
4. Ahn, J., and Prives, C. (2001) The C-terminus of p53: the more you learn the less you know. *Nat. Struct. Biol.* **8,** 730–732
5. Appella, E., and Anderson, C. W. (2001) Post-translational modifications and activation of p53 by genotoxic stresses. *Eur. J. Biochem.* **268,** 2764–2772
6. Di Lello, P., Jenkins, L. M. M., Jones, T. N., Nguyen, B. D., Hara, T., Yamaguchi, H., Dikeakos, J. D., Appella, E., Legault, P., and Omichinski, J. G. (2006) Structure of the Tfb1/p53 complex: Insights into the interaction between the p62/Tfb1 subunit of TFIIH and the activation domain of p53. *Mol. Cell* **22,** 731–740
7. Gu, W., and Roeder, R. G. (1997) Activation of p53 sequence-specific DNA binding by acetylation of the p53 C-terminal domain. *Cell* **90,** 595–606
8. Sakaguchi, K., Herrera, J. E., Saito, S., Miki, T., Bustin, M., Vassilev, A., Anderson, C. W., and Appella, E. (1998) DNA damage activates p53 through a phosphorylation-acetylation cascade. *Genes Dev.* **12,** 2831–2841
9. Krummel, K. A., Lee, C. J., Toledo, F., and Wahl, G. M. (2005) The C-terminal lysines fine-tune P53 stress responses in a mouse model but are not required for stability control or transactivation. *Proc. Natl. Acad. Sci. U. S. A.* **102,** 10188–10193
10. Feng, L., Lin, T., Uranishi, H., Gu, W., and Xu, Y. (2005) Functional analysis of the roles of posttranslational modifications at the p53 C terminus in regulating p53 stability and activity. *Mol. Cell. Biol.* **25,** 5389–5395
11. Liu, L., Scolnick, D. M., Trievel, R. C., Zhang, H. B., R., M., Halazonetis, T. D., and Berger, S. L. (1999) p53 sites acetylated in vitro by PCAF and p300 are acetylated in vivo in response to DNA damage. *Mol. Cell. Biol.* **19,** 1202–1209
12. Li, X., Wong, J., Tsai, S. Y., Tsai, M. J., and O'Malley, B. W. (2003) Progesterone and glucocorticoid receptors recruit distinct coactivator complexes and promote distinct patterns of local chromatin modification. *Mol. Cell. Biol.* **23,** 3763–3773
13. Ogryzko, V. V., Kotani, T., Zhang, X., Schiltz, R. L., Howard, T., Yang, X. J., Howard, B. H., Qin, J., and Nakatani, Y. (1998) Histone-like TAFs within the PCAF histone acetylase complex. *Cell* **94,** 35–44
14. Terui, T., Murakami, K., Takimoto, R., Takahashi, M., Takada, K., Murakami, T., Minami, S., Matsunaga, T., Takayama, T., Kato, J., and Niitsu, Y.

15. (2003) Induction of PIG3 and NOXA through acetylation of p53 at 320 and 373 lysine residues as a mechanism for apoptotic cell death by histone deacetylase inhibitors. *Cancer Res.* **63,** 8948–8954
15. Chao, C., Wu, Z., Mazur, S. J., Borges, H., Rossi, M., Lin, T., Wang, J. Y. J., Anderson, C. W., Appella, E., and Xu, Y. (2006) Acetylation of mouse p53 at lysine 317 negatively regulates p53 apoptotic activities after DNA damage. *Mol. Cell. Biol.* **26,** 6859–6869
16. Knights, C. D., Catania, J., Di Giovanni, S., Muratoglu, S., Perez, R., Swartzbeck, A., Quong, A. A., Zhang, X., Beerman, T., Pestell, R. G., and Avantaggiati, M. L. (2006) Distinct p53 acetylation cassettes differentially influence gene-expression patterns and cell fate. *J. Cell Biol.* **173,** 533–544
17. Abida, W. M., Nikolaev, A., Zhao, W., Zhang, W., and Gu, W. (2007) FBXO11 promotes the Neddylation of p53 and inhibits its transcriptional activity. *J. Biol. Chem.* **282,** 1797–1804
18. Le Cam, L., Linares, L. K., Paul, C., Julien, E., Lacroix, M., Hatchi, E., Triboulet, R., Bossis, G., Shmueli, A., Rodriguez, M. S., Coux, O., and Sardet, C. (2006) E4F1 is an atypical ubiquitin ligase that modulates p53 effector functions independently of degradation. *Cell* **127,** 775–788
19. Keller, A., Nesvizhskii, A. I., Kolker, E., and Aebersold, R. (2002) Empirical statistical model to estimate the accuracy of peptide identifications made by MS/MS and database search. *Anal. Chem.* **74,** 5383–5392
20. Li, X.-J., Zhang, H., Ranish, J. R., and Aebersold, R. (2003) Automated statistical analysis of protein abundance ratios from data generated by stable isotope dilution and tandem mass spectrometry. *Anal. Chem.* **75,** 6648–6657
21. Nesvizhskii, A. I., Keller, A., Kolker, E., and Aebersold, R. (2003) A statistical model for identifying proteins by tandem mass spectrometry. *Anal. Chem.* **75,** 4646–4658
22. Al-Shahrour, F., Minguez, P., Tarraga, J., Medina, I., Alloza, E., Montaner, D., and Dopazo, J. (2007) FatiGO +: a functional profiling tool for genomic data. Integration of functional annotation, regulatory motifs and interaction data with microarray experiments. *Nucleic Acids Res.* **35,** W91–W96
23. Al-Shahrour, F., Minguez, P., Tarraga, J., Montaner, D., Alloza, E., Vaquerizas, J. M., Conde, L., Blaschke, C., Vera, J., and Dopazo, J. (2006) BABELOMICS: a systems biology perspective in the functional annotation of genome-scale experiments. *Nucleic Acids Res.* **34,** W472–W476
24. Wheeler, D. L., Church, D. M., Federhen, S., Lash, A. E., Madden, T. L., Pontius, J. U., Schuler, G. D., Schriml, L. M., Sequeira, E., Tatusova, T. A., and Wagner, L. (2003) Database resources of the National Center for Biotechnology. *Nucleic Acids Res.* **31,** 28–33
25. Chiang, M. C., Juo, C. G., Chang, H. H., Chen, H. M., Yi, E. C., and Chern, Y. (2007) Systematic uncovering of multiple pathways underlying the pathology of Huntington disease by an acid-cleavable isotope-coded affinity tag approach. *Mol. Cell. Proteomics* **6,** 781–797
26. Puthier, D., Joly, F., Irla, M., Saade, M., Victorero, G., Loriod, B., and Nguyen, C. (2004) A general survey of thymocyte differentiation by transcriptional analysis of knockout mouse models. *J. Immunol.* **173,** 6109–6118
27. Clarke, A. R., Purdie, C. A., Harrison, D. J., Morris, R. G., Bird, C. C., Hooper, M. L., and Wyllie, A. H. (1993) Thymocyte apoptosis induced by p53-dependent and independent pathways. *Nature* **362,** 849–852
28. Lowe, S. W., Schmitt, E. M., Smith, S. W., Osborne, B. A., and Jacks, T. (1993) p53 is required for radiation-induced apoptosis in mouse thymocytes. *Nature* **362,** 847–849
29. Daoud, S. S., Munson, P. J., Reinhold, W., Young, L., Prabhu, V. V., Yu, Q., LaRose, J., Kohn, K. W., Weinstein, J. N., and Pommier, Y. (2003) Impact of p53 knockout and topotecan treatment on gene expression profiles in human colon carcinoma cells: a pharmacogenomic study. *Cancer Res.* **63,** 2782–2793
30. Ho, J. S., Ma, W., Mao, D. Y., and Benchimol, S. (2005) p53-dependent transcriptional repression of c-myc is required for G1 cell cycle arrest. *Mol. Cell. Biol.* **25,** 7423–7431
31. Guo, Q. M., Malek, R. L., Kim, S., Chiao, C., He, M., Ruffy, M., Sanka, K., Lee, N. H., Dang, C. V., and Liu, E. T. (2000) Identification of c-myc responsive genes using rat cDNA microarray. *Cancer Res.* **60,** 5922–5928
32. Louro, I. D., Bailey, E. C., Li, X., South, L. S., McKie-Bell, P. R., Yoder, B. K., Huang, C. C., Johnson, M. R., Hill, A. E., Johnson, R. L., and Ruppert, J. M. (2002) Comparative gene expression profile analysis of GLI and

c-MYC in an epithelial model of malignant transformation. *Cancer Res.* **62,** 5867–5873

33. Shiio, Y., Donohoe, S., Yi, E. C., Goodlett, D. R., Aebersold, R., and Eisenman, R. N. (2002) Quantitative proteomic analysis of Myc oncoprotein function. *EMBO J.* **21,** 5088–5096

34. Mourtada-Maarabouni, M., Kirkham, L., Jenkins, B., Rayner, J., Gonda, T. J., Starr, R., Trayner, I., Farzaneh, F., and Williams, G. T. (2003) Functional expression cloning reveals proapoptotic role for protein phosphatase 4. *Cell Death Differ.* **10,** 1016–1024

35. Im, C. N., Lee, J. S., Zheng, Y., and Seo, J. S. (2007) Iron chelation study in a normal human hepatocyte cell line suggests that tumor necrosis factor receptor-associated protein 1 (TRAP1) regulates production of reactive oxygen species. *J. Cell. Biochem.* **100,** 474–486

36. Masuda, Y., Shima, G., Aiuchi, T., Horie, M., Hori, K., Nakajo, S., Kajimoto, S., Shibayama-Imazu, T., and Nakaya, K. (2004) Involvement of tumor necrosis factor receptor-associated protein 1 (TRAP1) in apoptosis induced by β-hydroxyisovalerylshikonin. *J. Biol. Chem.* **279,** 42503–42515

37. Chen, F., Kamradt, M., Mulcahy, M., Byun, Y., Xu, H., McKay, M. J., and Cryns, V. L. (2002) Caspase proteolysis of the cohesin component RAD21 promotes apoptosis. *J. Biol. Chem.* **277,** 16775–16781

38. Sahara, S., Aoto, M., Eguchi, Y., Imamoto, N., Yoneda, Y., and Tsujimoto, Y. (1999) Acinus is a caspase-3-activated protein required for apoptotic chromatin condensation. *Nature* **401,** 168–173

39. Srinivasula, S. M., Fernandes-Alnemri, T., Zangrilli, J., Robertson, N., Armstrong, R. C., Wang, L., Trapani, J. A., Tomaselli, K. J., Litwack, G., and Alnemri, E. S. (1996) The Ced-3/interleukin 1β converting enzyme-like homolog Mch6 and the lamin-cleaving enzyme Mch2α are substrates for the apoptotic mediator CPP32. *J. Biol. Chem.* **271,** 27099–27106

40. Ashwell, J. D., Lu, F. W., and Vacchio, M. S. (2000) Glucocorticoids in T cell development and function. *Annu. Rev. Immunol.* **18,** 309–345

41. Liang, S.-H., and Clarke, M. F. (2001) Regulation of p53 localization. *Eur. J. Biochem.* **268,** 2779–2783

42. Kawaguchi, Y., Ito, A., Appella, E., and Yao, T.-P. (2006) Charge modification at multiple C-terminal lysine residues regulates p53 oligomerization and its nucleus-cytoplasm trafficking. *J. Biol. Chem.* **281,** 1394–1400

43. Orphanides, G., Wu, W. H., Lane, W. S., Hampsey, M., and Reinberg, D. (1999) The chromatin-specific transcription elongation factor FACT comprises human SPT16 and SSRP1 proteins. *Nature* **400,** 284–288

44. Landais, I., Lee, H., and Lu, H. (2006) Coupling caspase cleavage and ubiquitin-proteasome-dependent degradation of SSRP1 during apoptosis. *Cell Death Differ.* **13,** 1866–1878

45. Medenbach, J., Schreiner, S., Liu, S., Luhrmann, R., and Bindereif, A. (2004) Human U4/U6 snRNP recycling factor p110: mutational analysis reveals the function of the tetratricopeptide repeat domain in recycling. *Mol. Cell. Biol.* **24,** 7392–7401

46. Di Giovanni, S., Knights, C. D., Rao, M., Yakovlev, A., Beers, J., Catania, J., Avantaggiati, M. L., and Faden, A. I. (2006) The tumor suppressor protein p53 is required for neurite outgrowth and axon regeneration. *EMBO J.* **25,** 4084–4096

47. Sheikh, M. S., Carrier, F., Johnson, A. C., Ogdon, S. E., and Fornace, A. J., Jr. (1997) Identification of an additional p53-responsive site in the human epidermal growth factor receptor gene promotor. *Oncogene* **15,** 1095–1101

48. Alaoui-Jamali, M. A., Song, D. J., Benlimame, N., Yen, L., Deng, X., Hernandez-Perez, M., and Wang, T. (2003) Regulation of multiple tumor microenvironment markers by overexpression of single or paired combinations of ErbB receptors. *Cancer Res.* **63,** 3764–3774

49. Ohlsson, C., Kley, N., Werner, H., and LeRoith, D. (1998) p53 regulates insulin-like growth factor-I (IGF-I) receptor expression and IGF-I-induced tyrosine phosphorylation in an osteosarcoma cell line: interaction between p53 and Sp1. *Endocrinology* **139,** 1101–1107

50. Loughran, G., Huigsloot, M., Kiely, P. A., Smith, L. M., Floyd, S., Ayllon, V., and O'Connor, R. (2005) Gene expression profiles in cells transformed by overexpression of the IGF-I receptor. *Oncogene* **24,** 6185–6193

51. Alikhani, M., Alikhani, Z., He, H., Liu, R., Popek, B. I., and Graves, D. T. (2003) Lipopolysaccharides indirectly stimulate apoptosis and global induction of apoptotic genes in fibroblasts. *J. Biol. Chem.* **278,** 52901–52908

52. Ribardo, D. A., Crowe, S. E., Kuhl, K. R., Peterson, J. W., and Chopra, A. K. (2001) Prostaglandin levels in stimulated macrophages are controlled by phospholipase A2-activating protein and by activation of phospholipase C and D. *J. Biol. Chem.* **276,** 5467–5475

53. Cappellen, D., Luong-Nguyen, N. H., Bongiovanni, S., Grenet, O., Wanke, C., and Susa, M. (2002) Transcriptional program of mouse osteoclast differentiation governed by the macrophage colony-stimulating factor and the ligand for the receptor activator of NFκB. *J. Biol. Chem.* **277,** 21971–21982

54. Costa-Pereira, A. P., Tininini, S., Strobl, B., Alonzi, T., Schlaak, J. F., Is'harc, H., Gesualdo, I., Newman, S. J., Kerr, I. M., and Poli, V. (2002) Mutational switch of an IL-6 response to an interferon-γ-like response. *Proc. Natl. Acad. Sci. U. S. A.* **99,** 8043–8047

55. Feldmann, M., and Maini, R. N. (2001) Anti-TNFα therapy of rheumatoid arthritis: what have we learned? *Annu. Rev. Immunol.* **19,** 163–196

56. Liang, C. P., and Tall, A. R. (2001) Transcriptional profiling reveals global defects in energy metabolism, lipoprotein, and bile acid synthesis and transport with reversal by leptin treatment in ob/ob mouse liver. *J. Biol. Chem.* **276,** 49066–49076

57. Takahashi, N., Waelput, W., and Guisez, Y. (1999) Leptin is an endogenous protective protein against the toxicity exerted by tumor necrosis factor. *J. Exp. Med.* **189,** 207–212

58. Vanden Berghe, W., De Bosscher, K., Boone, E., Plaisance, S., and Haegeman, G. (1999) The nuclear factor-κB engages CBP/p300 and histone acetyltransferase activity for transcriptional activation of the interleukin-6 gene promoter. *J. Biol. Chem.* **274,** 32091–32098

59. Margetts, P. J., Kolb, M., Yu, L., Hoff, C. M., Holmes, C. J., Anthony, D. C., and Gauldie, J. (2002) Inflammatory cytokines, angiogenesis, and fibrosis in the rat peritoneum. *Am. J. Pathol.* **160,** 2285–2294

60. Chambers, R. C., Leoni, P., Kaminski, N., Laurent, G. J., and Heller, R. A. (2003) Global expression profiling of fibroblast responses to transforming growth factor-β1 reveals the induction of inhibitor of differentiation-1 and provides evidence of smooth muscle cell phenotypic switching. *Am. J. Pathol.* **162,** 533–546

61. Shi-wen, X., Stanton, L. A., Kennedy, L., Pala, D., Chen, Y., Howat, S. L., Renzoni, E. A., Carter, D. E., Bou-Gharios, G., Stratton, R. J., Pearson, J. D., Beier, F., Lyons, K. M., Black, C. M., Abraham, D. J., and Leask, A. (2006) CCN2 is necessary for adhesive responses to transforming growth factor-β1 in embryonic fibroblasts. *J. Biol. Chem.* **281,** 10715–10726

62. Saile, B., Matthes, N., El Armouche, H., Neubauer, K., and Ramadori, G. (2001) The bcl, NFκB and p53/p21WAF1 systems are involved in spontaneous apoptosis and in the anti-apoptotic effect of TGF-β or TNF-α on activated hepatic stellate cells. *Eur. J. Cell Biol.* **80,** 554–561

63. Ladiwala, U., Li, H., Antel, J. P., and Nalbantoglu, J. (1999) p53 induction by tumor necrosis factor-α and involvement of p53 in cell death of human oligodendrocytes. *J. Neurochem.* **73,** 605–611

64. Brown, J., Ongusaha, P. P., Kim, H. G., Nuti, S., Mandinova, A., Lee, J. W., Khosravi-Far, R., Aaronson, S. A., and Lee, S. W. (2007) CDIP, a novel pro-apoptotic gene, regulates TNFα-mediated apoptosis in a p53-dependent manner. *EMBO J.* **26,** 3410–3422

65. Tuckermann, J. P., Kleiman, A., McPherson, K. G., and Reichardt, H. M. (2005) Molecular mechanisms of glucocorticoids in the control of inflammation and lymphocyte apoptosis. *Crit. Rev. Clin. Lab. Sci.* **42,** 71–104

66. Stocklin, E., Wissler, M., Gouilleux, F., and Groner, B. (1996) Functional interactions between Stat5 and the glucocorticoid receptor. *Nature* **383,** 726–728

67. Caldenhoven, E., Liden, J., Wissink, S., Van de Stolpe, A., Raaijmakers, J., Koenderman, L., Okret, S., Gustafsson, J. A., and Van der Saag, P. T. (1995) Negative cross-talk between RelA and the glucocorticoid receptor: a possible mechanism for the antiinflammatory action of glucocorticoids. *Mol. Endocrinol.* **9,** 401–412

68. Sengupta, S., Vonesch, J.-L., Waltzinger, C., Zheng, H., and Wasylyk, B. (2000) Negative cross-talk between p53 and the glucocorticoid receptor and its role in neuroblastoma cells. *EMBO J.* **19,** 6051–6064

69. Sengupta, S., and Wasylyk, B. (2001) Ligand-dependent interaction of the glucocorticoid receptor with p53 enhances their degradation by Hdm2. *Genes Dev.* **15,** 2367–2380